Journal Pre-proofs

3D printing tablets for high-precision dose titration of caffeine

Liam Krueger, Yuxue Cao, Zheng Zheng, Jason Ward, Jared A. Miles, Amirali Popat

PII: S0378-5173(23)00552-5
DOI: https://doi.org/10.1016/j.ijpharm.2023.123132
Reference: IJP 123132

To appear in: *International Journal of Pharmaceutics*

Received Date: 20 March 2023
Revised Date: 6 June 2023
Accepted Date: 8 June 2023

Please cite this article as: L. Krueger, Y. Cao, Z. Zheng, J. Ward, J.A. Miles, A. Popat, 3D printing tablets for high-precision dose titration of caffeine, *International Journal of Pharmaceutics* (2023), doi: https://doi.org/10.1016/j.ijpharm.2023.123132

3D printing tablets for high-precision dose titration of caffeine

Liam Krueger, Yuxue Cao, Zheng Zheng, Jason Ward, Jared A. Miles*, Amirali Popat*

School of Pharmacy, The University of Queensland, Woolloongabba, QLD 4102, Australia

Abstract

Through 3D printing (3DP), many parameters of solid oral dosage forms can be customised, allowing for truly personalised medicine in a way that traditional pharmaceutical manufacturing would struggle to achieve. One of the many options for customisation involves dose titration, allowing for gradual weaning of a medication at dose intervals smaller than what is available commercially. . In this study we demonstrate the high accuracy and precision of 3DP a caffeine dose titration, selected due to its global prevalence as a behavioural drug and well-known titration-dependent adverse reactions in humans. This was achieved using a simple filament base of polyvinyl alcohol, glycerol, and starch, utilising hot melt extrusion coupled with fused deposition modelling 3DP. Tablets containing 25 mg, 50 mg, and 100 mg doses of caffeine were successfully printed with drug content in the accepted range prescribed for conventional tablets (90 – 110%), and excellent precision whereby the weights of all doses showed a relative standard deviation of no more than 3%. Importantly, these results proved 3D printed tablets to be far superior to splitting a commercially available caffeine tablet. Additional assessment of filament and tablet samples were reviewed by differential scanning calorimetry, thermogravimetric analysis, HPLC, and scanning electron microscopy, showing no evidence of degradation of caffeine or the raw materials, with smooth and consistent filament extrusion. Upon dissolution, all tablets achieved greater than 70% release between 50-60 minutes, showing a predictable rapid release profile regardless of dose. The outcomes of this study highlight the benefits that dose titration with 3DP can offer, especially to more commonly prescribed medications that can have even more harmful withdrawal-induced adverse events.

1. Introduction

3D printing (3DP) generally involves building a three-dimensional object in a layer-by-layer fashion, and while initially developed for rapid industrial prototyping, the technology has also garnered interest for healthcare and pharmaceutical applications[1, 2]. In recent years, 3DP to create solid oral dosage forms has advanced rapidly. The first 3D printed tablet, Spritam®[3], saw U.S. Food & Drug Administration (FDA) approval in 2015, followed by investigational new drug (IND) approval for three products (T19, T20 and T21) over 2021-22[4]. 3DP medicines most commonly use biocompatible thermoplastic polymers in which drugs can be loaded to produce customised doses, release profiles, or aesthetics, and can be printed on-site for the patient[5]. While there are many different types of 3DP, one of the most common is hot melt extrusion (HME) coupled to fused deposition modelling (FDM), a well-researched and reliable process outlined in Scheme 1[6-9].

The use cases of 3DP compared to conventional manufacturing cover many different themes, a notable one being the ability to precisely change the dose of medication at will[10]. New studies continue to show remarkable progress in 3DP technologies, formulations, and analytical techniques, but can be lacking in the selection of clinically relevant active pharmaceutical ingredients (APIs), or the accuracy and precision of the printed dosage forms. For example, oral dosage forms containing calcein[11] and fluorescein[12] are useful for a proof-of-concept model, but not as therapeutic agents. Many studies have used clinically relevant APIs which could benefit from personalised dosing, but often are printed at subtherapeutic doses [13-16]. A select few studies have indeed used 3DP with clinically relevant APIs specifically for dose titration, which have shown excellent accuracy and precision[17, 18]. The main limitations of these studies include a comparatively lower drug loading between 1-10%, as well as unpredictable or unmodifiable drug release rates, where dissolution of the highest dose tablet was at least two hours longer than the lowest[17, 18]. These factors could present challenges when working with APIs that need fast or otherwise predictable release rates over a wider dose range.

Therefore, in this study, 3DP is used to address the clinical problem of difficulties with dose titration. Caffeine was chosen as a clinically relevant drug due to its known side effect profile when abruptly decreasing dose, and subsequently its clinical applicability for personalised dose titration. In the United States alone it has been reported that nearly 90% of adults consume a high dose of caffeine daily[19]. The incidence and severity of caffeine withdrawal symptoms worsen with larger and more abrupt dose reductions[20], and there are many opportunities for human error to take place when attempting to slowly wean the dose of a medication. This could include selecting the wrong dose of tablets, or simply by the inherent process of splitting tablets, which is known to have considerable inaccuracies even when the tablets are scored[21]. This highlights an urgent need for developing and studying the dose titration of clinically relevant drugs which will in turn fast track the progress of clinically available 3D printed medications. Caffeine has previously been used in FDM[22-24], pressure-assisted syringe[25], stereolithography[14] and inkjet[26] 3DP studies, showing that it is not only an appropriate example of a drug requiring dose titration, but also that it is widely compatible with 3DP.

The process outlined in Scheme 1 was used to melt caffeine into a polymer-based filament that can then be 3D printed. Unlike many other studies, tablet dimensions were varied to target a specified weight and therefore dose, as would be done in a clinical setting, as opposed to aiming for a predetermined tablet size and producing an arbitrary dose of the

active ingredient. By optimising the filament formulation and other parameters such as operating temperatures speeds, reliable and high-quality filament was obtained which in turn was able to be 3D printed with ease. The processes outlined in Scheme 1 were optimised, allowing for the production of filament with commercial-grade accuracy, and tablets with strong mechanical properties that achieved 100% caffeine release in around 90 minutes without any degradation.

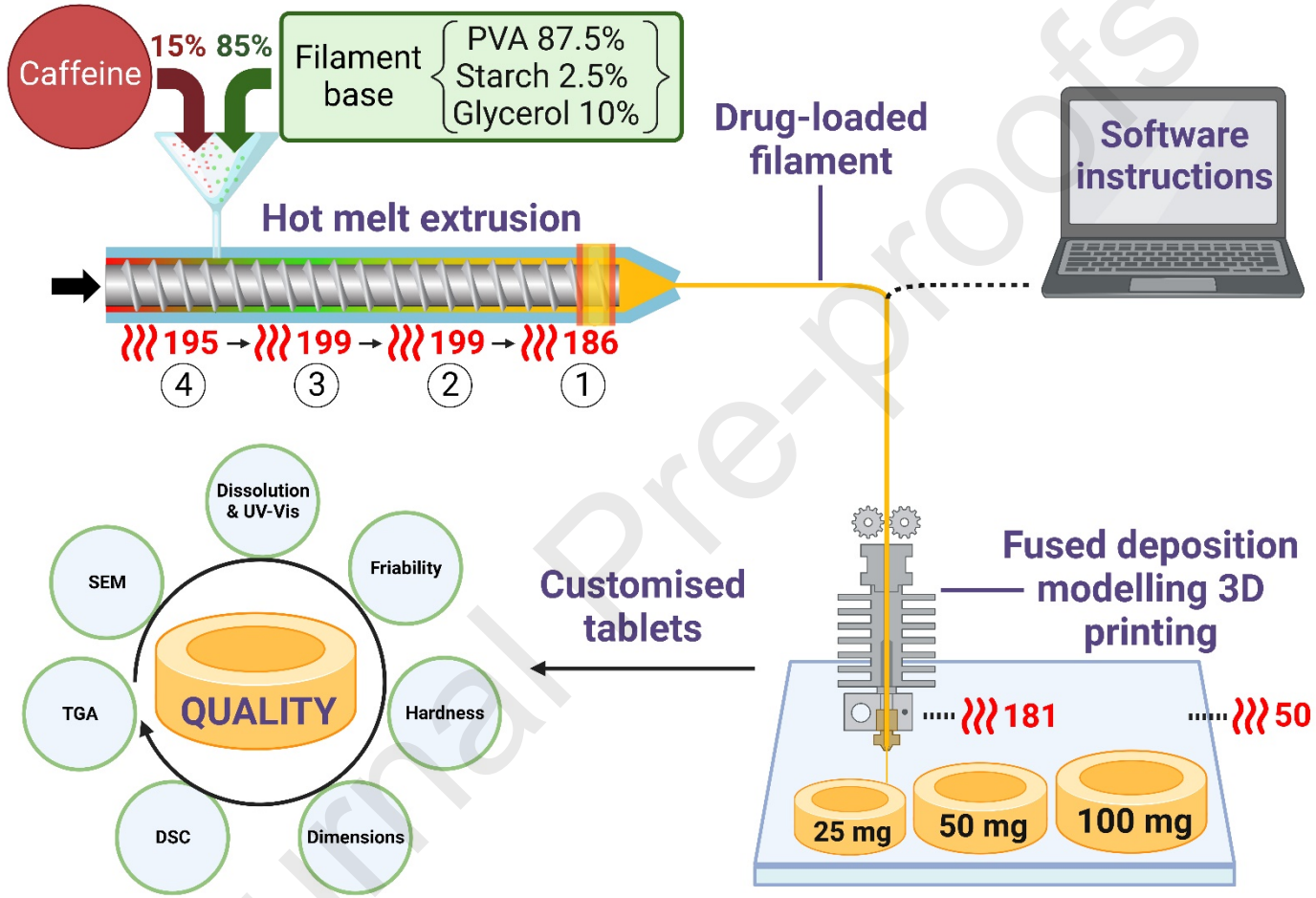

Scheme 1: The processes of converting raw materials into personalised 3D printed tablets. A polymeric base is combined with a chosen drug through HME, and the resulting filament is used to print tablets with variable features designated by instructions from slicing software. Printed tablets then undergo quality control assessment. Created with biorender.com.

2. Materials and Methods

2.1 Materials

Polyvinyl alcohol (PVA) (Mowiol® 4-88, MW 31000, 81381-1KG), starch (potato, soluble, S-2004) and caffeine (anhydrous, 99%, W222402-1KG-K) were obtained from Sigma-Aldrich. Glycerol was obtained from Gold Cross (ACT, Australia). All assays used analytical grade hydrochloric acid (HCl) from Merck (Darmstadt, Germany) and type II pure water.

2.2 Filament preparation

All components of the filament preparation were incorporated by mass as a % w/w. A blend of 87.5% PVA, 2.5% starch, and 10% glycerol, referred to as the filament base hereafter, was chosen due to its compatibility with HME/FDM processes in terms of flexibility, strength, and inter-layer adhesion. Caffeine was added to the filament base at 15% to produce a final formulation of 15% caffeine, 74.4% PVA, 2.1% starch, and 8.5% glycerol. Initially, all components of the formulation in their respective ratios were combined in a mortar and pestle to give a 300 g yield. The formulation was then dried in an oven at 50°C for four hours. Following this, the formulation was blended in a 1300 W Preethi XPRO DUO benchtop grinder (Chengalpattu, India) for one minute, then dried again for one hour. This process was repeated 2-3 times as necessary to remove aggregates and produce an evenly distributed powder. This powder was then dried overnight prior to HME.

2.3 Hot melt extrusion

A 3devo Composer 350 (3devo B.V., Utrecht, Netherlands) featuring twin screws, 3-stage compression and four individually controlled heating zones was used for HME of the powder formulation into filament for 3DP. The screw speed was set to 2.1 rpm and the temperatures used for each heating zone were 195°C at zone 4 (hopper), 199°C at zone 3, 199°C at zone 2, and 186°C at zone 1 (nozzle). Material was extruded through a standard 4 mm die, cooled by fans, and fed through an in-line optical filament diameter sensor by pulley wheels.

2.4 3D printing

The tablet geometries were designed by modifying the dimensions of a cylinder shape inserted from PrusaSlicer (version 2.5.0). The *in silico* dimensions were scaled to target final tablet weights of 0.17, 0.33 and 0.67 g. Additional details regarding the tablet dimensions and a graphical representation from PrusaSlicer can be found in Supporting Information Figure S1. Initial predictions for tablet weight were made using the default calculations in PrusaSlicer using the PLA profile (density 1.24 g/cm^3).

An unmodified Creality Ender 3 S1 was used to 3D print all tablets, utilising a 0.4 mm brass nozzle and a polycarbonate (PC) coated steel sheet for the print bed. The Creality Ender 3 S1 profile from PrusaSlicer was loaded with the ‘Generic PLA’ parameters, modified to use a nozzle temperature of 181°C and bed temperature of 50°C. Other minor modifications can be

found in Supporting Information Figure S2. The nozzle was primed with filament by initially loading with commercial polylactic acid (PLA) filament, then performing a 'cold pull' before loading with the drug-containing filament. This involves heating the nozzle to 220°C and extruding PLA, then allowing the nozzle to cool to 90°C before disengaging the extruder gears and removing the filament manually while it is soft, but not molten, effectively taking with it any previous filament or contaminants in the nozzle. A purge line was printed at the beginning of each batch as per the default slicer settings. Up to 9 tablets were printed in each batch, distributed evenly across the print bed with the draft shield setting enabled.

2.5 Differential scanning calorimetry and thermogravimetric analysis

A Mettler Toledo TGA/DSC2 STAR^e System (Mettler Toledo, Oregon, United States) was used to perform differential scanning calorimetry (DSC) and thermogravimetric analysis (TGA). Samples of 5-10 mg of PVA, caffeine, starch, glycerol, as well as crushed samples of the drug-loaded filaments, physical mixtures, and tablets, were placed into an Alumina 70 µL open pan and heated from 25°C to 800°C at a rate of 10°C/min. Air was used as the purge gas. STARe v16.10 was used for data analysis and DSC and TGA thermogram generation.

2.6 Scanning electron microscopy

A JSM-7100F Field Emission Scanning Electron Microscope (JEOL, Japan) was used to perform scanning electron microscopy (SEM) to observe the surface morphologies of the filament and tablets. Samples were platinum coated and viewed at a voltage of 2.0 kW (filament) or 5.0 kW (tablet).

2.7 Physical characterisation of tablets

Dimensional accuracy was measured along the tablet X, Y and Z axes using a digital calliper (accuracy ± 0.2 mm) with a sample size of 10 tablets. A Logan Instruments FAB-2S friability tester (New Jersey, USA) was used to assess the 3D printed tablets against the requirements for conventional tablets per the British Pharmacopoeia (BP). 10 tablets of each dose were randomly selected and weighed before tumbling in the friability tester for 4 minutes at a speed of 25 rpm. The total percentage weight loss of the tablets was then calculated. An Erweka GmbH D-63150 hardness tester (Heusenstamm, Germany) was used to assess the breaking force in Newtons (N) along the X and Y axes of three tablets of each dose.

2.8 Content assay, uniformity of content and *in vitro* dissolution

A Varian VK 7000 dissolution apparatus (North Carolina, USA) was used to assess the release of caffeine from 3D printed tablets over time. For each dose, three tablets were placed into separate wells containing 900 mL of 0.1 M HCl at 37°C, and constantly stirred at 50 rpm. 5 mL samples were withdrawn through a 10 µM full flow filter (Agilent Technologies, 161017-372) at predetermined times, and immediately replaced with fresh solvent.

Commercial 200 mg caffeine tablets (Futurevits, Cheshire, UK) were split into halves, quarters, and eighths (n = 3) with a tablet cutter. Each tablet fragment was fully dissolved in a known volume of solvent before an aliquot was centrifuged at 15000 rpm to remove insoluble excipients.

The caffeine content of samples was determined via a GENESYS 50 UV-Visible spectrophotometer (Thermo Fisher Scientific, USA) using a UV quartz cuvette with a path length of 1 cm. Initially, caffeine powder was dissolved in 0.1 M HCl and scanned to determine the λ_{max} (272 nm) for all future analyses. A calibration curve ranging from 0.002 mg/mL to 0.02 mg/mL ($r^2 = 0.999$) was developed by diluting three independent samples with solvent (refer to Supporting Information Figure S3.1 for a representative calibration curve). Similarly, samples from *in vitro* dissolution were analysed and diluted with 0.1 M HCl if necessary to fall within the calibration curve.

Mathematical models were applied to the dissolution graphs to observe the best fit for these tablets using the DDSolver add-in for Microsoft Excel[27]. The release models tested were zero-order, first-order, Hixson-Crowell, Korsmeyer-Peppas, and Higuchi, the calculations for which can be found in Supporting Information Figure S4.

High-performance liquid chromatography (HPLC) was used for drug content assay, uniformity of content, and the identification of any potential degradation of caffeine during HME or 3DP. The analysis of caffeine was carried out using UHPLC 1260 infinity (Agilent Technologies) with a Kinetex® 5µm C18 column (pore size 100 Å, size 250 x 4.6 mm) at room temperature with a detection wavelength of 272 nm. The mobile phase consisted of a mixture of methanol and water (40:60, v/v) and injection volume of 10 µL. A calibration curve ranging from 0.004 mg/mL to 0.5 mg/mL ($r^2 = 1$) was developed by diluting three independent samples with solvent (refer to Supporting Information Figure S3.2 for a representative calibration curve). To perform a drug content assay and a uniformity of content analysis as outlined in the BP, 10 tablets each of the 25 mg, 50 mg and 100 mg doses were fully dissolved in 50 mL of type II pure water and samples were centrifuged at 15000 rpm for 15 minutes. The supernatant was then diluted in the solvent to fall within the calibration curve and analysed for caffeine content and any possible degradation.

3. Results and Discussion

3.1 Raw materials characterisation

To assess the suitability of caffeine and other excipients for HME and 3DP, DSC and TGA were initially conducted on the raw materials to observe thermal characteristics, including the identification of glass transitions, crystallinity, melting points, and degradation temperatures (Figure 1). Analysis of raw PVA showed a peak at around 90°C, similar to other reports of its glass transition temperature (T_g)[28, 29], and again at its melting point (T_m), observed here around 193°C. Caffeine showed a strong peak around 237°C, consistent with its melting point[23, 30]. Glycerol showed a broad peak around 285°C at its reported boiling point[31]. The thermal properties of starch are known to vary widely based on factors such as its origin and water content[32], however in this experiment broad T_g and T_m peaks are observed around 70°C and 260°C respectively. Since all components appeared to be compatible below the proposed processing temperatures, it was expected that the mixture would create a filament comprised of the molten PVA and glycerol as a base, homogenised with caffeine and starch in their crystalline or amorphous forms.

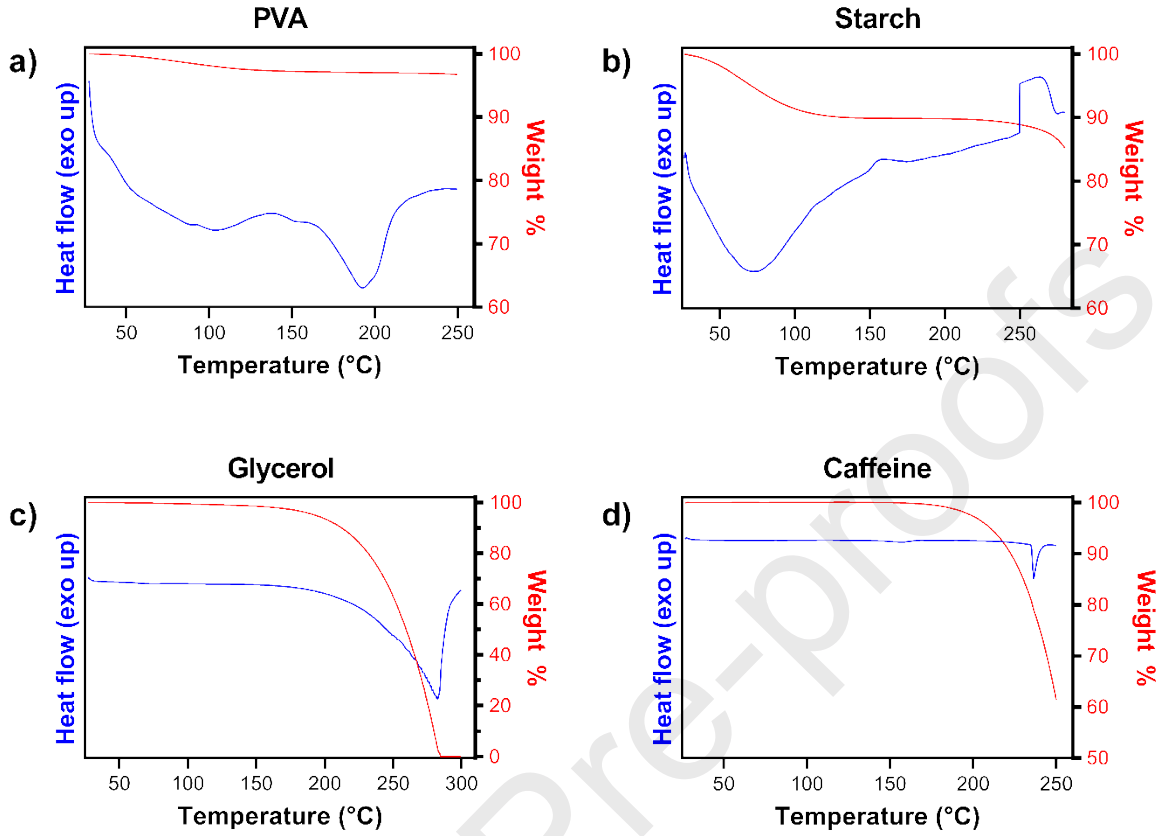

Figure 1: DSC (blue) and TGA (red) thermograms of the raw materials. a): PVA; b): starch; c): glycerol; d): caffeine. Distinct endothermic peaks are visible for the T_g and T_m of PVA, T_g and T_m of starch, boiling point of glycerol, and T_m of caffeine.

3.2 Hot melt extrusion

The first step towards producing 3D printed caffeine tablets was to extrude drug-loaded filament using HME. PVA was chosen for the main matrix-forming polymer due to its water solubility, biocompatibility, and known suitability for HME and FDM processing[33-35]. Preliminary results of filament made with raw PVA were too brittle for FDM printing, a problem that has been encountered in previous studies[36, 37]. Adding a plasticiser to improve this is common, and glycerol was chosen as this combination has previously been successfully extruded and printed [34, 35, 38]. In the experimental stage, formulations with higher amounts of glycerol inhibited the flowability through the extruder and led to overly flexible filament. Conversely, those with lower amounts of glycerol were not flexible enough to be spooled, or otherwise could be broken by the extruder drive gears of the 3D printer. The selected formulation containing 10% glycerol gave the ideal flexibility, and the addition of starch benefitted the formulation not only due to its plasticising effect with PVA, but also by aiding flowability as a lubricant. The method of combining PVA, glycerol and starch is well-researched and very commonly used to make films in the context of food preparation or packaging[39].

The temperatures used for HME had to be monitored closely, especially in the final heating zone near the die, to stabilise the extrusion temperature. The overarching variable for the ideal extrusion temperature is the main matrix-forming polymer, and the properties of the polymer itself, such as the molecular weight. The physical and thermal properties of PVA vary greatly with molecular weight, but similar results regarding extrusion temperatures were found between the type of PVA used in this experiment (Mowiol® 4-88, viscosity ~4 mPas[40]) and a similar grade (Gohensol™ EG 05P; viscosity ~5.3 mPas[41]), which has been plasticised with glycerol at 5% and 15% by weight for extrusion at 190°C and 175°C, respectively[35, 38]. In our study, deviations as little as 3°C too low would produce excessively brittle filament, or too high would produce filament too molten to hold a consistent diameter. Further adjustments to the formulation may have been able to widen the compatible temperature range, making the filament less sensitive to minor changes and more reproducible. Ultimately, HME with a 186°C nozzle temperature at 2.1 rpm screw speed gave the best quality filament. In-line measurements from the HME optical sensor showed that the extruded filament had a mean diameter of 1.75 mm and standard deviation of 0.07 mm, falling between the generally accepted 3DP industry standard of 1.75 ± 0.1 mm. Exact readings exported from the optical sensor (one reading per second) can be found in Supporting Information Figure S5.

DSC and TGA was conducted to allow for comparison between the raw materials, physical mixture, and samples of the filament and tablets (Figure 3). In the filament, the T_g and T_m peaks of raw PVA, observed previously at 90°C and 190°C, shifted to roughly 70°C and 170°C. This could be due to the presence of other materials, especially with the prominent plasticising effects of starch and glycerol [42]. It can be observed that the T_g is significantly more pronounced in the filament compared to the physical mixture, as the process of HME is likely the main contributing factor allowing the other materials to combine homogenously with the PVA. For example, it has been stated that starch can broaden the melting range and slightly lower the T_m of PVA, due to decreasing its crystallinity by incorporation of the amorphous starch[43]. Similarly, in the presence of glycerol, even in small amounts of 0.5 – 2.0% w/w, it has been found that the melting range can be broadened, the onset of thermal degradation increased, and the T_m decreased[44].

The peak for the T_m of caffeine is not present in the physical mixture or the filament (Figure 3), indicating that it is either present in an amorphous form or dissolved in the mixture. Caffeine has previously been reported to be stable below 200°C[45], and a previous study using caffeine with FDM has suggested that since the HME and FDM processes were performed below the melting point of caffeine, it likely remains crystalline unless solubilised by the molten polymer[23].

SEM images of the cross-section of the filament reveal a highly porous structure (Figure 2). A magnified image of a pore in Figure 2b shows fibrous material within. A potential explanation for the fibrous appearance inside the pores could be the presence of starch. If the starch is not miscible within the molten PVA, it is possible that the starch has been dispersed throughout the PVA matrix, but not necessarily solubilised within it. However, it has been hypothesised in other experiments that if a mixture of two polymers shares a single T_g in between the T_g of the individual polymers, then it can be inferred that the mixture is miscible[46]. In this experiment the distinct peak for the T_g of PVA, observed at around 90°C, was not visible in the filament sample, and rather there was one single peak around 70°C. Other studies that have incorporated larger proportions of starch with PLA shows what could be described as a rough surface, but more homogenous and not fibrous as it appears in

this experiment[47, 48]. An alternative to the origin of the fibrous material could be the presence of the API. One study compared a drug-free PVA filament to one with 4% drug loading, where a noticeably rougher surface could be observed[49], especially from a lateral view, though not necessarily porous. Lateral views of the filament produced here can be found in Supporting Information Figure S6. The comparatively higher drug loading here could explain the less homogenous appearance of the filament cross-section. Another study using a PVA-based filament with 30% loading of mesoporous magnesium carbonate produced a highly porous filament cross-section, though fibres or crystals do not appear to present as was the case here[50]. Other studies that have used a similar formulation for the base filament, consisting of PVA and glycerol, do not display SEM images and thus comparisons about the porosity of this filament specifically is difficult[35, 38].

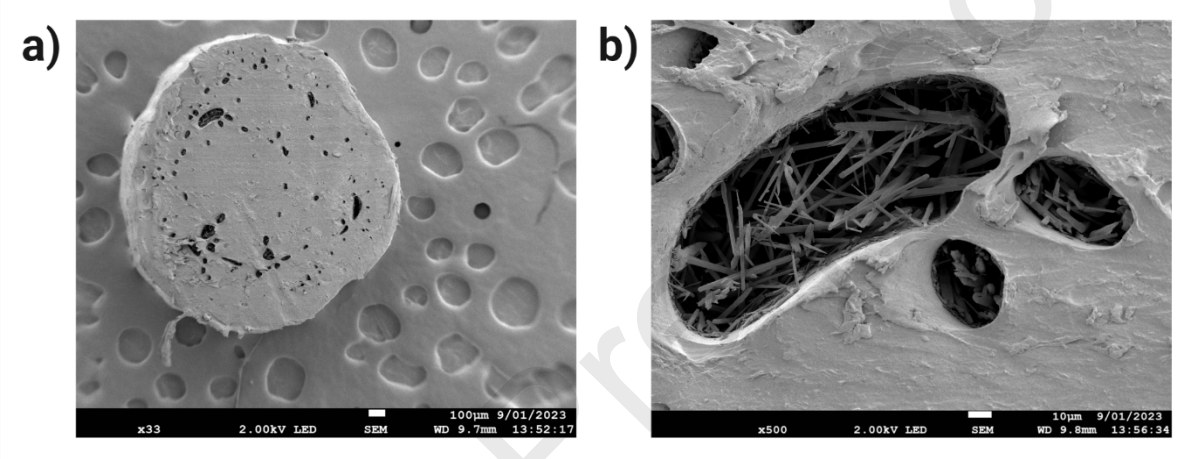

Figure 2: SEM imaging of filament produced by HME. a): cross-section of filament; b): increased magnification of pores observed within the filament, wherein fibrous material can be seen.

3.3 3D printing

After production of the filament, tablets were designed *in silico* such that the final weights would yield doses of 25 mg, 50 mg, and 100 mg of caffeine, accounting for the drug loading of 15%. These dimensions were estimated based on calculations generated by PrusaSlicer 3D printing software, which considers the volume of the object and the density of the material. In this experiment, the default PLA profile was used which assumes a density of 1.24g/cm^3, as the true density of the experimental formulation was not calculated. The grade of PVA used is quoted as 1.3 g/cm^3 as per the safety data sheet[40], higher than that of PLA. Indeed, in preliminary trials it was found that printed objects consistently weighed higher than the generated *in silico* predictions. For this reason, tablet sizes were chosen such that the estimated weight would be lower than the true target weight of the tablets.

The tablet geometry was customised with the goal of obtaining an immediate release profile. The design featured one vertical perimeter/shell, one bottom layer and one top layer. This was done with the intention of allowing the dissolution media to flow rapidly through the partially hollow core of the tablet, for maximal surface area exposure, after dissolving only one solid layer. Targeting a release profile by modifying a tablet in this way has become common practice in pharmaceutical 3DP, and it is highly effective yet simple to

implement[49, 51-54]. However, it has been reported that high infill levels used with a swellable polymer cause the pores to block and therefore during dissolution the tablet can behave more as a solid than as a partially hollow object[53]. Therefore, a 50% grid infill was chosen for a high surface area-to-volume (SA:V) ratio without risking excessive pore swelling.

As with HME, the temperature used for printing had to be controlled precisely. Variations of greater than 2°C from the set temperature of 181°C would cause under-extrusion and clogging if too low, or over-extrusion and stringing from the nozzle if too high. Furthermore, the ideal printing temperature being lower than the extrusion temperature is unusual, and the opposite would be expected for any HME/FDM pairing. The reason for this is not certain, especially as later DSC and TGA results do not appear to show any explicit changes between the filament and tablet samples. Regardless, at the set temperature of 181°C there were no signs of under-extrusion or nozzle clogs observed during printing.

The DSC and TGA thermograms of the tablet appear to be almost identical to the physical mixture and filament samples in terms of the locations and shapes of peaks (Figure 3). Compared to the filament, the T_g of the tablet sample remained around 70°C, but the T_m appears to have shifted from 170°C in the filament up to about 180°C. A potential explanation for this could be the degradation of glycerol. The highest temperature that the materials are exposed to is 199°C during HME, and while PVA and starch were observed to be stable, this temperature appears to be where the degradation curve of both caffeine and glycerol begin (Figure 1). While a shallow peak for glycerol was observed in the filament, it cannot be seen in the tablet sample (Figure 3). It is unclear whether this can be interpreted as degradation, or if it could be that this subsequent process of melting and extruding the filament through the 3D printer has allowed the PVA and glycerol to combine more homogenously. As with the filament sample, the peak for caffeine was not visible.

The operating temperatures being close to the degradation temperatures of glycerol and caffeine may be a concern for the thermal stability of the formulation. However, for caffeine in particular, content assays discussed later showed no evidence of significant caffeine loss due to degradation when compared to the theoretical dose, and this was confirmed using HPLC analysis.

Interestingly, the physical mixture and the samples of filament and tablet do not show any suggestive evidence of degradation until around 250°C. It was hypothesised in this experiment that HME successfully produced a consistent and homogenous mixture of all ingredients, and therefore the stability of the mixture is more important than the stability of the raw materials.

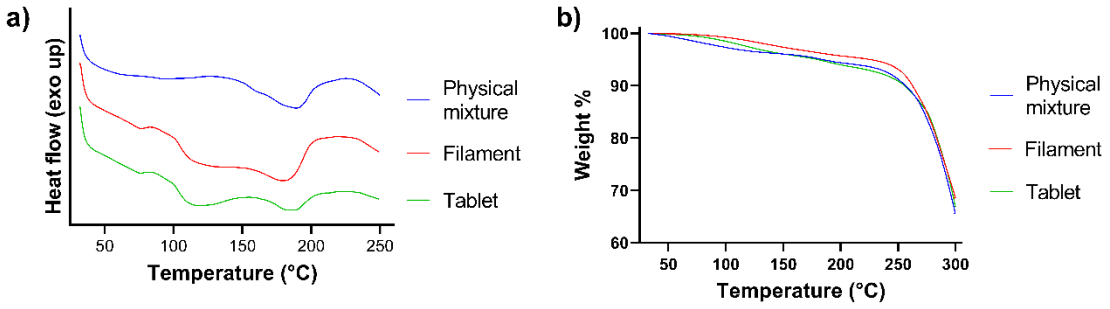

Figure 3: DSC (a) and TGA (b) thermograms of samples of the physical mixture of raw materials, filament produced by HME, and tablets produced by FDM. Endothermic peaks in the heat flow at about 70°C and 170-180°C can be seen, which are likely the T_g and T_m of the samples. Weight loss indicates that degradation begins around 250°C.

SEM images of the tablet grid infill pattern and first layer surface show a high accuracy (Figure 4), representing adequate parameters of the HME and FDM processes. Imaging of the first layer (Figure 4b) shows the surface of the tablet on the side that is in contact with the build plate, with a relatively smooth surface and the absence of extrusion lines. This indicates that 181°C was an appropriate temperature for printing, slightly higher than the T_m of 170°C shown in the DSC data of the filament, and allowed for the extruded filament to melt and combine homogenously along the extrusion path.

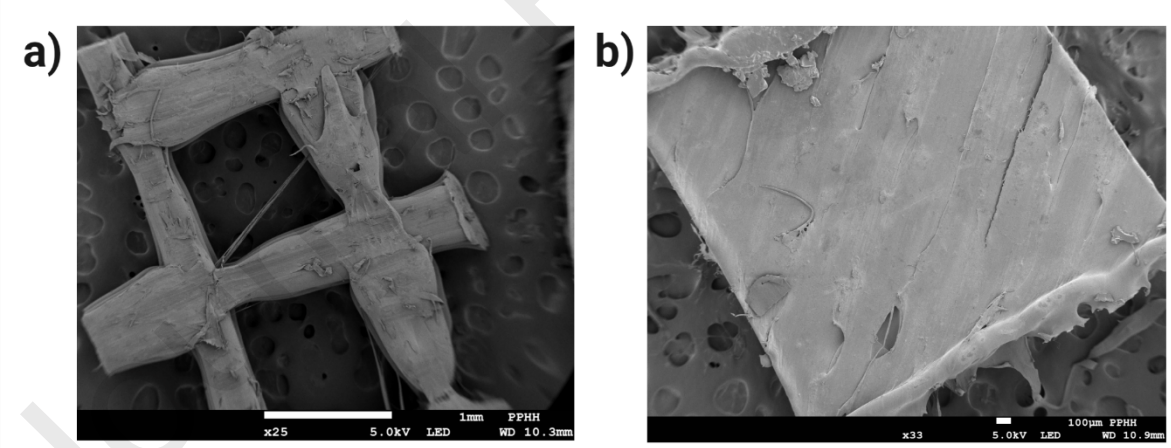

Figure 4: SEM images of 3D printed tablets. a): cross-section view of grid infill pattern of 3D printed tablet; b): surface of the first layer of a tablet (in contact with the build plate).

3.4 Physical characterisation of tablets

All tablets were found to have high quality physical characteristics as shown in Table 1. The measured dimensions of the tablets adhered very closely with the dimensions set in the PrusaSlicer 3DP software. Additionally, all tablets showed no friability and satisfactory

hardness. Although there are no official standards for hardness, it is generally accepted that tablets, excluding chewable or orodispersible dosage forms, should have a hardness over 4 kg (~39 N).

Table 1: Physical characteristics of dimensional accuracy (n = 10), friability (n = 10), and hardness (n = 3) of 3D printed tablets.

Target dose	Total variation from *in silico* dimensions (Mean ± SD %)	X-axis hardness (N; Mean ± SD)	Y-axis hardness (N; Mean ± SD)
25 mg	0.89 ± 0.81%	159 ± 27	116 ± 25
50 mg	0.12 ± 0.66%	213 ± 42	206 ± 49
100 mg	-0.34 ± 0.59%	213 ± 15	230 ± 21

3.5 Weight variation

The weight of the 25 mg, 50 mg, and 100 mg tablets, in a batch of 47 tablets of each strength, deviated from the target weight by -2.4%, -6.6% and -5.7%, respectively (Supporting Information Table S7.1). However, all strengths had a very high precision shown by the relative standard deviation of less than 3%. This indicates that the confounding factor may lie not with the processes of extrusion or printing, but rather with the tablet design that dictates the weights of the tablets. Since the tablets weighed less than desired, scaling could increase the dose accuracy while retaining the high precision. The weight estimation that is generated in the slicing software is based on the density of the selected filament profile, and with a custom filament blend of unknown density the correlation between the estimated weight and true weight is imperfect. Nevertheless, BP requirements for tablets of a mass over 250 mg require that no more than two tablets in a batch of 20 deviate from the average mass by more than 5% [55], which all tablets comply with (Supporting Information Table S7.2).

3.6 Content assay, uniformity of content and i*n vitro* dissolution

Initially, 10 tablets of each dose were analysed by HPLC to find their mean dose as part of the drug content assay, followed by calculating the deviation of each tablet from the mean for the uniformity of content. The tablets yielded mean doses of 25.1 mg, 49.5 mg, and 103.6 mg, corresponding to 100.4%, 99.0%, and 103.6% of the target doses, respectively (Supporting information Table S8). This complies with BP specifications that the average content must be between 95 and 105% of the stated amount [55]. Importantly, it was also demonstrated that no tablet deviated from the mean by more than 10%, which successfully

meets the BP criteria for uniformity of content [55](Supporting information Table S8). The dose being within acceptable limits suggests that caffeine did not undergo any significant degradation at the elevated processing temperatures, and HPLC analysis confirmed this. Dissolved filament and tablet samples had only one distinct peak (Supporting Information Figure S3.3), showing no degradation products.

Building upon the data collected from the weights and drug content of the 3D printed tablets, there is the potential to adjust the scaling of individual tablet sizes to achieve even better precision. Indeed, the accuracy and precision of the 3D printed tablets far exceeded the traditional method of titrating caffeine by splitting commercially available tablets. Unscored 200 mg caffeine tablets were split with a tablet-cutter into halves, quarters, and eighths in an attempt to achieve 100 mg, 50 mg, and 25 mg doses, respectively. All split tablet fragments contained significantly less caffeine than the target dose (-21% to -29%) and showed a high amount of variation between fragments, with a standard deviation at least five times greater than the 3D printed equivalent (Supporting Information Table S9.1). This clearly demonstrates the superiority of the 3DP method used here regarding both accuracy and precision of dosing.

Dissolution of the 3D printed tablets was then carried out in 0.1 M HCl to study the release characteristics in a simulated gastric environment (Figure 5). All tablets demonstrate a high dose accuracy (Figure 5a), where the 25 mg, 50 mg, and 100 mg tablets (n = 3 for each dose) deviated from their target dose by only 2.5%, -3.9%, and -0.37% respectively (Supporting Information Table S9.2).

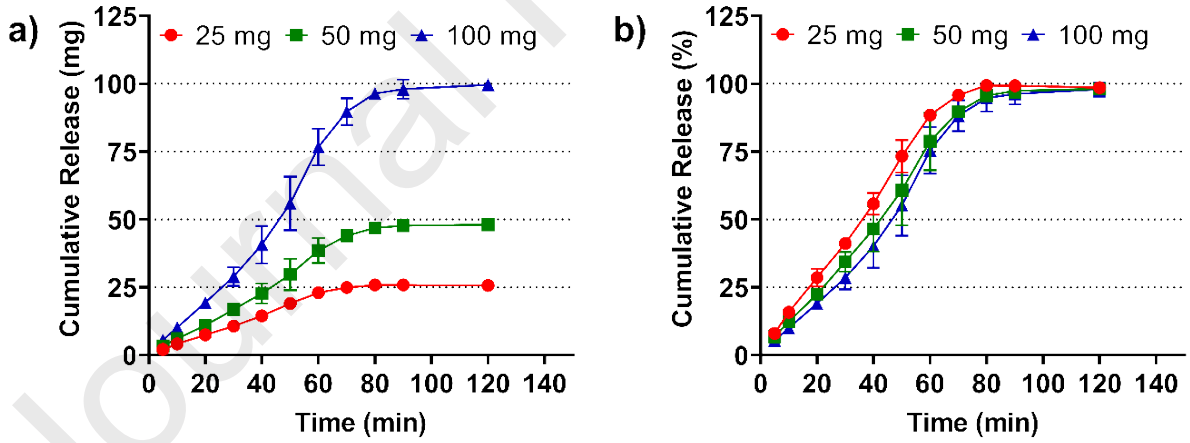

Figure 5: *In vitro* dissolution of 3D printed caffeine tablets of 25 mg, 50 mg, and 100 mg doses in 0.1M HCl over 120 minutes a): cumulative release in mg; b): % cumulative release. Each point refers to mean ± SD (n = 3).

The immediate release *in silico* tablet design proved to be effective, as rapid caffeine release was seen in all three tablet types with ~70% of total drug release between 50-60 minutes (Figure 5b). Tablets of the lowest dose (25 mg) showed slightly faster release amongst all groups, which would be expected due to smaller tablets inherently having a higher SA:V

ratio[56]. At the 60-minute point, the 50 mg and 100 mg tablets had reached 79% and 75%, respectively, whereas the 25 mg tablets reached a similar level about 5-10 minutes earlier, showing 73% release at 50 minutes. Given the vast difference in doses, this small variation in release appears insignificant and shows that the method of having a fixed infill geometry with a variable tablet size is a very reliable technique to change the dose without affecting the release profile. This is an important advantage upon comparison to other studies using HME and FDM for dose titration that used either a variable infill, or completely solid tablets where in either case the release rate of the highest dose tablet was about two hours slower than the lowest dose[17, 18]. In one study the addition of up to 16% w/w of a disintegrant, or designing the tablet to contain channels did not significantly increase the dissolution rate[17], which is an interesting finding and exemplifies how significant the impact of tablet geometry can be for release profiles. In our study, all tablets showed ~100% caffeine release within 90 minutes, confirming the consistency and reliability of our approach. This rapid release from these tablets is attributed to high solubility of caffeine, the infill design, and the effect of starch. Although not meeting the criteria for immediate release as per the BP, whereby not less than 70% has been released after 45 minutes, the data showing full release in ~90 minutes is still best described as immediate or rapid. Based on the dissolution data we are confident that the tablets will provide the intended rapid release of caffeine at the expected dose.

The dissolution of caffeine from all 3D printed tablets most closely followed the Hixson-Crowell model, where the r^2 values for the 25 mg, 50 mg and 100 mg doses were 0.96, 0.94 and 0.93, respectively (Supporting Information Figure S4). The Hixson-Crowell model is seldom used for 3D printed tablets in existing literature as opposed to other models such as first-order or Korsmeyer-Peppas. Experiments using FDM 3DP that identified a good fit with this model used a 100% printing infill[57, 58], and therefore factors such as the SA:V ratio would be comparable to conventionally manufactured tablets, and vastly different to this study where a 50% infill was used. The Hixson-Crowell model describes drug release from an eroding tablet as being limited by dissolution velocity rather than by diffusion of the drug through the polymer matrix[58]. Other studies that use a lower infill density to create a partially hollow tablet have found the best fit with the Korsmeyer-Peppas model, but it should be noted that the Hixson-Crowell was not tested in these studies[56, 59]. Interestingly, in another study it was determined that the first-order model was the best fit for 3D prints with a mesh and ring geometry, but the Higuchi model was the best fit for solid tablets[60]. These findings exemplify the complexity of predicting drug release from 3D printed tablets when considering additional variables such as internal tablet geometries and the individual characteristics of the chosen polymer used to deliver the API. Predictions of release profiles using SA:V ratios shows promise, but more studies are needed to validate this model[58].

4. Conclusion

This study demonstrates the potential of 3D printing in creating customised dosage forms for high-precision dose titration of caffeine. The results show that 3D printed tablets at doses of 25 mg, 50 mg, and 100 mg achieved physical properties and release characteristics (>75% release in less than 60 minutes in 0.1 M HCl) that are predictable, consistent, and of a sufficient quality to meet the standards set for conventionally manufactured tablets. Furthermore, the stability of caffeine was preserved even with processing temperatures of up to 199°C validated by uniformity of content analysis. The precision and accuracy of the data

gathered here suggest that doses can accurately be chosen simply by scaling the tablets, while attempting to do the same by splitting commercial tablets results in significantly varied drug content. With further research and development, 3D printing could reform the dosing procedures for medications susceptible to severe titration-dependent side effects by providing patients with more accurate and precise dosages tailored to their individual needs.

Author contributions

L.K.: conceptualisation, methodology, investigation, data collection, data analysis, writing – original draft preparation.

Y.C.: data collection, data curation, data analysis, writing – review and editing.

Z.Z.: data collection, writing – review and editing.

J.W.: data collection.

J.M.: writing – review and editing, methodology, data analysis, data curation, supervision and funding acquisition.

A.P.: writing – review and editing, methodology, data analysis, data curation, supervision and funding acquisition.

Acknowledgements

The authors acknowledge funding from the School of Pharmacy, The University of Queensland.

The authors acknowledge the facilities, and the scientific and technical assistance, of the Australian Microscopy & Microanalysis Research Facility at the Centre for Microscopy and Microanalysis, The University of Queensland.

Special thanks to Nisha Tyagi for assistance with performing DSC/TGA analyses.

Special thanks to Taskeen Janjua for assistance with performing HPLC analysis.

Conflict of interest

The authors declare no conflict of interest.

References

[1] S.J. Trenfield, A. Awad, C.M. Madla, G.B. Hatton, J. Firth, A. Goyanes, S. Gaisford, A.W. Basit, Shaping the future: recent advances of 3D printing in drug delivery and healthcare, Expert Opinion on Drug Delivery, 16 (2019) 1081-1094.

[2] L. Krueger, J.A. Miles, A. Popat, 3D printing hybrid materials using fused deposition modelling for solid oral dosage forms, Journal of Controlled Release, 351 (2022) 444-455.

[3] U.S. Food & Drug Administration, Spritam (levetiracetam) tablets. Accessed 2022 Apr 12 from https://www.accessdata.fda.gov/drugsatfda_docs/nda/2015/207958Orig1s000TOC.cfm#:~:text=Approval%20Date%3A%2007%2F31%2F2015, in, 2016 May 27.

[4] TRIASTEK, ABOUT TRIASTEK. Accessed 2022 Oct 25 from https://www.triastek.com/, in, 2022.

[5] A. Awad, A. Yao, S.J. Trenfield, A. Goyanes, S. Gaisford, A.W. Basit, 3D Printed Tablets (Printlets) with Braille and Moon Patterns for Visually Impaired Patients, Pharmaceutics, 12 (2020) 172.

[6] J. Macedo, N.F. da Costa, V. Vanhoorne, C. Vervaet, J.F. Pinto, The Precision and Accuracy of 3D Printing of Tablets by Fused Deposition Modelling, Journal of Pharmaceutical Sciences, 111 (2022) 2814-2826.

[7] J. Zhang, X. Feng, H. Patil, R.V. Tiwari, M.A. Repka, Coupling 3D printing with hot-melt extrusion to produce controlled-release tablets, International Journal of Pharmaceutics, 519 (2017) 186-197.

[8] S. Bandari, D. Nyavanandi, N. Dumpa, M.A. Repka, Coupling hot melt extrusion and fused deposition modeling: Critical properties for successful performance, Advanced Drug Delivery Reviews, 172 (2021) 52-63.

[9] W. Jamróz, M. Kurek, J. Szafraniec-Szczęsny, A. Czech, K. Gawlak, J. Knapik-Kowalczuk, B. Leszczyński, A. Wróbel, M. Paluch, R. Jachowicz, Speed it up, slow it down…An issue of bicalutamide release from 3D printed tablets, European Journal of Pharmaceutical Sciences, 143 (2020) 105169.

[10] L. Krueger, J.A. Miles, K.J. Steadman, T. Kumeria, C.R. Freeman, A. Popat, 3D printing: potential clinical applications for personalised solid dose medications, Medical Journal of Australia, (2022).

[11] T. Tagami, N. Nagata, N. Hayashi, E. Ogawa, K. Fukushige, N. Sakai, T. Ozeki, Defined drug release from 3D-printed composite tablets consisting of drug-loaded polyvinylalcohol and a water-soluble or water-insoluble polymer filler, International Journal of Pharmaceutics, 543 (2018) 361-367.

[12] A. Goyanes, A.B.M. Buanz, A.W. Basit, S. Gaisford, Fused-filament 3D printing (3DP) for fabrication of tablets, International Journal of Pharmaceutics, 476 (2014) 88-92.

[13] J. Zhang, W. Yang, A.Q. Vo, X. Feng, X. Ye, D.W. Kim, M.A. Repka, Hydroxypropyl methylcellulose-based controlled release dosage by melt extrusion and 3D printing: Structure and drug release correlation, Carbohydrate Polymers, 177 (2017) 49-57.

[14] P. Robles-Martinez, X. Xu, S.J. Trenfield, A. Awad, A. Goyanes, R. Telford, A.W. Basit, S. Gaisford, 3D Printing of a Multi-Layered Polypill Containing Six Drugs Using a Novel Stereolithographic Method, Pharmaceutics, 11 (2019) 274.

[15] R.C.R. Beck, P.S. Chaves, A. Goyanes, B. Vukosavljevic, A. Buanz, M. Windbergs, A.W. Basit, S. Gaisford, 3D printed tablets loaded with polymeric nanocapsules: An innovative approach to produce customized drug delivery systems, International Journal of Pharmaceutics, 528 (2017) 268-279.

[16] J. Krause, M. Bogdahn, F. Schneider, M. Koziolek, W. Weitschies, Design and characterization of a novel 3D printed pressure-controlled drug delivery system, European Journal of Pharmaceutical Sciences, 140 (2019) 105060.

[17] S. Henry, L. De Vadder, M. Decorte, S. Francia, M. Van Steenkiste, J. Saevels, V. Vanhoorne, C. Vervaet, Development of a 3D-Printed Dosing Platform to Aid in Zolpidem Withdrawal Therapy, Pharmaceutics, 13 (2021) 1684.

[18] J. Macedo, R. Marques, C. Vervaet, J.F. Pinto, Production of Bi-Compartmental Tablets by FDM 3D Printing for the Withdrawal of Diazepam, Pharmaceutics, 15 (2023) 538.

[19] C.D. Frary, R.K. Johnson, M.Q. Wang, Food sources and intakes of caffeine in the diets of persons in the United States, Journal of the American Dietetic Association, 105 (2005) 110-113.

[20] S.M. Evans, R.R. Griffiths, Caffeine Withdrawal: A Parametric Analysis of Caffeine Dosing Conditions, Journal of Pharmacology and Experimental Therapeutics, 289 (1999) 285.

[21] E. van Santen, D.M. Barends, H.W. Frijlink, Breaking of scored tablets: a review, European Journal of Pharmaceutics and Biopharmaceutics, 53 (2002) 139-145.

[22] H. Wang, N. Dumpa, S. Bandari, T. Durig, M.A. Repka, Fabrication of Taste-Masked Donut-Shaped Tablets Via Fused Filament Fabrication 3D Printing Paired with Hot-Melt Extrusion Techniques, American Association of Pharmaceutical Scientists PharmSciTech, 21 (2020) 243.

[23] E. Fuenmayor, M. Forde, A.V. Healy, D.M. Devine, J.G. Lyons, C. McConville, I. Major, Comparison of fused-filament fabrication to direct compression and injection molding in the manufacture of oral tablets, International Journal of Pharmaceutics, 558 (2019) 328-340.

[24] A. Goyanes, J. Wang, A. Buanz, R. Martínez-Pacheco, R. Telford, S. Gaisford, A.W. Basit, 3D Printing of Medicines: Engineering Novel Oral Devices with Unique Design and Drug Release Characteristics, Molecular Pharmaceutics, 12 (2015) 4077-4084.

[25] W.J. Goh, S.X. Tan, G. Pastorin, P.C.L. Ho, J. Hu, S.H. Lim, 3D printing of four-in-one oral polypill with multiple release profiles for personalized delivery of caffeine and vitamin B analogues, International Journal of Pharmaceutics, 598 (2021) 120360.

[26] N. Sandler, A. Määttänen, P. Ihalainen, L. Kronberg, A. Meierjohann, T. Viitala, J. Peltonen, Inkjet printing of drug substances and use of porous substrates-towards individualized dosing, Journal of Pharmaceutical Sciences, 100 (2011) 3386-3395.

[27] Y. Zhang, M. Huo, J. Zhou, A. Zou, W. Li, C. Yao, S. Xie, DDSolver: An Add-In Program for Modeling and Comparison of Drug Dissolution Profiles, The AAPS Journal, 12 (2010) 263-271.

[28] E. Fathi, N. Atyabi, M. Imani, Z. Alinejad, Physically crosslinked polyvinyl alcohol–dextran blend xerogels: Morphology and thermal behavior, Carbohydrate Polymers, 84 (2011) 145-152.

[29] PubChem, Polyvinyl alcohol. Accessed 2023 Jan 27 from https://pubchem.ncbi.nlm.nih.gov/compound/Polyvinyl-alcohol, in, 2005 March 26.

[30] PubChem, Caffeine. Accessed 2022 Dec 28 from https://pubchem.ncbi.nlm.nih.gov/compound/Caffeine, in, 2004 Sep 16.

[31] PubChem, Glycerol. Accessed 2023 Jan 04 from https://pubchem.ncbi.nlm.nih.gov/compound/Glycerol, in, 2004 Sep 16.

[32] P. Liu, L. Yu, H. Liu, L. Chen, L. Li, Glass transition temperature of starch studied by a high-speed DSC, Carbohydrate Polymers, 77 (2009) 250-253.

[33] M.A. Azad, D. Olawuni, G. Kimbell, A.Z.M. Badruddoza, M.S. Hossain, T. Sultana, Polymers for Extrusion-Based 3D Printing of Pharmaceuticals: A Holistic Materials-Process Perspective, Pharmaceutics, 12 (2020).

[34] A. Melocchi, M. Uboldi, F. Briatico-Vangosa, S. Moutaharrik, M. Cerea, A. Foppoli, A. Maroni, L. Palugan, L. Zema, A. Gazzaniga, The Chronotopic™ System for Pulsatile and Colonic Delivery of Active Molecules in the Era of Precision Medicine: Feasibility by 3D Printing via Fused Deposition Modeling (FDM), Pharmaceutics, 13 (2021) 759.

[35] A. Melocchi, M. Uboldi, N. Inverardi, F. Briatico-Vangosa, F. Baldi, S. Pandini, G. Scalet, F. Auricchio, M. Cerea, A. Foppoli, A. Maroni, L. Zema, A. Gazzaniga, Expandable drug delivery system for gastric retention based on shape memory polymers: Development via 4D printing and extrusion, International Journal of Pharmaceutics, 571 (2019) 118700.

[36] M. Alhijjaj, P. Belton, S. Qi, An investigation into the use of polymer blends to improve the printability of and regulate drug release from pharmaceutical solid dispersions prepared via fused deposition modeling (FDM) 3D printing, European Journal of Pharmaceutics and Biopharmaceutics, 108 (2016) 111-125.

[37] S. Palekar, P.K. Nukala, S.M. Mishra, T. Kipping, K. Patel, Application of 3D printing technology and quality by design approach for development of age-appropriate pediatric formulation of baclofen, International Journal of Pharmaceutics, 556 (2019) 106-116.

[38] A. Melocchi, F. Parietti, A. Maroni, A. Foppoli, A. Gazzaniga, L. Zema, Hot-melt extruded filaments based on pharmaceutical grade polymers for 3D printing by fused deposition modeling, International Journal of Pharmaceutics, 509 (2016) 255-263.

[39] R. Abedi-Firoozjah, N. Chabook, O. Rostami, M. Heydari, A. Kolahdouz-Nasiri, F. Javanmardi, K. Abdolmaleki, A. Mousavi Khaneghah, PVA/starch films: An updated review of their preparation, characterization, and diverse applications in the food industry, Polymer Testing, 118 (2023) 107903.

[40] Merck, MOWIOL® 4-88 Reagent SDS. Accessed 2023 Jan 27 from https://www.merckmillipore.com/AU/en/product/msds/EMD_BIO-475904?Origin=PDP, in, 2022 Dec 15.

[41] Mitsubishi Chemical Corporation, High Purity PVOH EG Series. Accessed 2023 Feb 12 from https://www.gohsenol.com/doc_e/spcl/spcl_01/spcl_08.shtml, in.

[42] L. Mao, S. Imam, S. Gordon, P. Cinelli, E. Chiellini, Extruded Cornstarch-Glycerol-Polyvinyl Alcohol Blends: Mechanical Properties, Morphology, and Biodegradability, Journal of Polymers and the Environment, 8 (2000) 205-211.

[43] G.-X. Zou, P.-Q. Jin, L.-Z. Xin, Extruded Starch/PVA Composites: Water Resistance, Thermal Properties, and Morphology, Journal of Elastomers & Plastics, 40 (2008) 303-316.

[44] M. Mohsin, A. Hossin, Y. Haik, Thermal and mechanical properties of poly(vinyl alcohol) plasticized with glycerol, Journal of Applied Polymer Science, 122 (2011) 3102-3109.

[45] R. Wang, J. Xue, L. Meng, J.-W. Lee, Z. Zhao, P. Sun, L. Cai, T. Huang, Z. Wang, Z.-K. Wang, Y. Duan, J.L. Yang, S. Tan, Y. Yuan, Y. Huang, Y. Yang, Caffeine Improves the Performance and Thermal Stability of Perovskite Solar Cells, Joule, 3 (2019) 1464-1477.

[46] N.G. Solanki, M. Tahsin, A.V. Shah, A.T.M. Serajuddin, Formulation of 3D Printed Tablet for Rapid Drug Release by Fused Deposition Modeling: Screening Polymers for Drug Release, Drug-Polymer Miscibility and Printability, Journal of Pharmaceutical Sciences, 107 (2018) 390-401.

[47] A. Haryńska, H. Janik, M. Sienkiewicz, B. Mikolaszek, J. Kucińska-Lipka, PLA–Potato Thermoplastic Starch Filament as a Sustainable Alternative to the Conventional PLA Filament: Processing, Characterization, and FFF 3D Printing, ACS Sustainable Chemistry & Engineering, 9 (2021) 6923-6938.

[48] Q. Ju, Z. Tang, H. Shi, Y. Zhu, Y. Shen, T. Wang, Thermoplastic starch based blends as a highly renewable filament for fused deposition modeling 3D printing, International Journal of Biological Macromolecules, 219 (2022) 175-184.

[49] A. Goyanes, P. Robles Martinez, A. Buanz, A.W. Basit, S. Gaisford, Effect of geometry on drug release from 3D printed tablets, International Journal of Pharmaceutics, 494 (2015) 657-663.

[50] C.S. Katsiotis, M. Åhlén, M. Strømme, K. Welch, 3D-Printed Mesoporous Carrier System for Delivery of Poorly Soluble Drugs, Pharmaceutics, 13 (2021) 1096.

[51] A. Goyanes, F. Fina, A. Martorana, D. Sedough, S. Gaisford, A.W. Basit, Development of modified release 3D printed tablets (printlets) with pharmaceutical excipients using additive manufacturing, International Journal of Pharmaceutics, 527 (2017) 21-30.

[52] B. Arafat, M. Wojsz, A. Isreb, R.T. Forbes, M. Isreb, W. Ahmed, T. Arafat, M.A. Alhnan, Tablet fragmentation without a disintegrant: A novel design approach for accelerating disintegration and drug release from 3D printed cellulosic tablets, European Journal of Pharmaceutical Sciences, 118 (2018) 191-199.

[53] T. McDonagh, P. Belton, S. Qi, An investigation into the effects of geometric scaling and pore structure on drug dose and release of 3D printed solid dosage forms, European Journal of Pharmaceutics and Biopharmaceutics, 177 (2022) 113-125.

[54] X. Zhao, W. Wei, R. Niu, Q. Li, C. Hu, S. Jiang, 3D Printed Intragastric Floating and Sustained-Release Tablets with Air Chambers, Journal of Pharmaceutical Sciences, 111 (2022) 116-123.

[55] British Pharmacopoeia, Appendix XII C. Consistency of Formulated Preparations. Accessed 2023 Feb 15 from https://www-pharmacopoeia-com.ezproxy.library.uq.edu.au/bp-2023/appendices/appendix-12/appendix-xii-c--consistency-of-formulated-preparations.html?date=2023-01-01#f20906, in, 2023 (11.0 update).

[56] M. Kyobula, A. Adedeji, M.R. Alexander, E. Saleh, R. Wildman, I. Ashcroft, P.R. Gellert, C.J. Roberts, 3D inkjet printing of tablets exploiting bespoke complex geometries for controlled and tuneable drug release, Journal of Controlled Release, 261 (2017) 207-215.

[57] K. Ilyés, N.K. Kovács, A. Balogh, E. Borbás, B. Farkas, T. Casian, G. Marosi, I. Tomuță, Z.K. Nagy, The applicability of pharmaceutical polymeric blends for the fused deposition modelling (FDM) 3D

technique: Material considerations–printability–process modulation, with consecutive effects on in vitro release, stability and degradation, European Journal of Pharmaceutical Sciences, 129 (2019) 110-123.

[58] H. Windolf, R. Chamberlain, J. Quodbach, Predicting Drug Release from 3D Printed Oral Medicines Based on the Surface Area to Volume Ratio of Tablet Geometry, Pharmaceutics, 13 (2021) 1453.

[59] M. Đuranović, S. Obeid, M. Madžarević, S. Cvijić, S. Ibrić, Paracetamol extended release FDM 3D printlets: Evaluation of formulation variables on printability and drug release, International Journal of Pharmaceutics, 592 (2021) 120053.

[60] S.A. Khaled, M.R. Alexander, D.J. Irvine, R.D. Wildman, M.J. Wallace, S. Sharpe, J. Yoo, C.J. Roberts, Extrusion 3D Printing of Paracetamol Tablets from a Single Formulation with Tunable Release Profiles Through Control of Tablet Geometry, American Association of Pharmaceutical Scientists PharmSciTech, 19 (2018) 3403-3413.

Author contributions

L.K.: conceptualisation, methodology, investigation, data collection, data analysis, writing – original draft preparation.

Y.C.: data collection, data curation, data analysis, writing – review and editing.

Z.Z.: data collection, writing – review and editing.

J.W.: data collection.

J.M.: writing – review and editing, methodology, data analysis, data curation, supervision and funding acquisition.

A.P.: writing – review and editing, methodology, data analysis, data curation, supervision and funding acquisition.

Declaration of interests

☐ The authors declare that they have no known competing financial interests or personal relationships that could have appeared to influence the work reported in this paper.

☒ The authors declare the following financial interests/personal relationships which may be considered as potential competing interests:

Amirali Popat and Jared Miles reports financial support was provided by University of Queensland.